International Journal of Bifurcation and Chaos, Vol. 8, No. 9 (1998) 1801–1809

SELF-PULSING AND CHAOS IN AN EXTENDED-CAVITY DIODE LASER WITH INTRACAVITY ATOMIC ABSORBER

F. DI TEODORO*, E. CERBONESCHI, D. HENNEQUIN† and E. ARIMONDO
INFM, Dipartimento di Fisica, Università di Pisa, Piazza Torricelli, 2, I-56126 Pisa, Italy

Received July 31, 1997; Revised January 12, 1998

An experimental investigation of the temporal dynamics of a diode laser subject to optical feedback from an external cavity containing a cell filled with cesium vapor has been performed. Peculiar dynamic regimes, such as self-pulsing, low-dimensional, and high-dimensional chaos, characterized by a new time scale, much longer than the time scales of all instabilities taking place in diode lasers under standard feedback conditions, have been identified.

1. Introduction

Diode lasers exposed to optical feedback from an external cavity containing an atomic absorber are systems of great interest in the fields of spectroscopy, atomic physics and quantum optics, as they provide stable sources, with very narrow linewidth, on resonance with atomic transition frequencies. In recent years, these systems were widely investigated, mainly for the purpose of improving the spectral performance of the lasers and achieving an absolute frequency stabilization [Cuneo *et al.*, 1994; Kitching *et al.*, 1994; Liu *et al.*, 1994]. On the contrary, there was no knowledge about the nonlinear dynamics and chaotic properties of these systems. In this paper, we provide a description of such properties and identify distinctive features of the dynamics related to the presence of the absorber.

We report on experimental investigations performed on an extended-cavity diode laser containing a cell filled with cesium vapor, in a saturation spectroscopy configuration [Schmidt *et al.*, 1994]. We focus on the temporal dynamics of the system, showing that the presence of the atomic absorber inside the feedback cavity produces characteristic dynamic regimes, which take place on a peculiar time scale, much longer than the time scales typical of the dynamics of laser diodes under standard feedback conditions. Starting from a stable operating regime characterized by self-locking of the laser frequency to the central Lamb dip of the saturated absorption spectrum of the Cs D_2 line, we have observed, with increasing detuning from the atomic resonance, a self-pulsing regime of the laser output in the form of a sequence of intensity dropouts and, eventually, a chaotic regime. Taking advantage of the fact that the dynamics of the system takes place on different time scales, spaced at least by three–four orders of magnitude, we have separated the slow dynamics induced by the absorber. Due to its long time scale, this dynamics is very easily accessible experimentally. The experimental time series have been analyzed with the time-delay method so as to reconstruct embedding portraits

*Current address: Physics Department, Bryn Mawr College, Bryn Mawr, PA 19010-2899 USA.
†Permanent address: Laboratoire de Spectroscopie Hertzienne, Unité associée au CNRS, Université des Sciences et Technologies de Lille, 59655 Villeneuve d'Ascq Cedex, France.

and recurrence plots. The attractors in the phase space of the laser system have been characterized quantitatively by computing the Lyapunov exponent spectrum and the correlation dimension. From this analysis, it turns out that the signal observed for large detuning from the atomic resonance shows high dimensional chaos, characterized by two positive Lyapunov exponents. This feature could either pertain to the hyperchaos [Rössler, 1979] or to the coexistence of different chaotic attractors. The dynamics, either periodic or chaotic, observed out of the locking range, within a certain range of detuning from the atomic resonance, is characterized by the long time scale mentioned above. This time scale is absent in the dynamics of laser diodes in the standard feedback set-up, and therefore, it identifies, among the operation regimes of the extended-cavity laser, those which are determined by the presence of the atomic absorber.

Extended-cavity diode lasers with intracavity atomic absorber have never been studied previously from the point of view of nonlinear dynamics. In [di Teodoro *et al.*, 1997], we discussed the spectral features of this system, pointing out that the presence of the absorber substantially modifies the mode pattern in the phase space of the extended-cavity laser. We also developed a rate equation model suitable for the interpretation of the spectral phenomena, which could not provide, however, a description of the global dynamics. In the absence of a comprehensive theoretical model for the system considered, the analysis performed here makes it possible to infer general information on the dynamics in the phase space from the measured time dependence of the laser emission.

This paper is organized as follows: In Sec. 2 we describe the experimental apparatus and the measurements performed. In Sec. 3 we illustrate the observed dynamic evolution of the laser emission and discuss the results of the time-series analysis. Conclusions and final remarks are presented in Sec. 4.

2. Experimental

The experimental setup is shown schematically in Fig. 1. The observations were performed using a Spectra Diode Laser SDL-5400. The laser was optically coupled, through an antireflection coated collimating objective, to an external cavity terminated by a diffraction grating, placed 46 cm from the laser. A 4 cm long cell containing Cs vapor at the equilibrium density at room temperature was inserted within the external cavity. A fraction of the laser intensity was extracted from the external cavity by means of a beam splitter with less than 10% reflectivity and used for the detection. To avoid unwanted feedback from optical surfaces in the measuring equipment, a magneto-optical isolator providing 40 dB of attenuation for counterpropagating light was placed on the path of the extracted beam. A scanning confocal Fabry–Perot spectrum analyzer, model 240 by Coherent, was used to detect the optical spectrum of the laser emission. Absolute optical frequency measurements were performed by comparing, with the spectrum analyzer, the laser frequency and the frequency of a reference diode laser. The reference laser was locked, through a standard technique of hybrid optical and electronic feedback, to the transition $F = 4 \rightarrow F' = 5$ of the Cs D_2 line. The temporal evolution of the output laser intensity was detected, simultaneously with the spectral measurements, by means of an avalanche photodiode with 1.2 GHz cutoff frequency. The photodiode signal was monitored with a Tektronix TDS540 digital oscilloscope, with 500 MHz bandwidth.

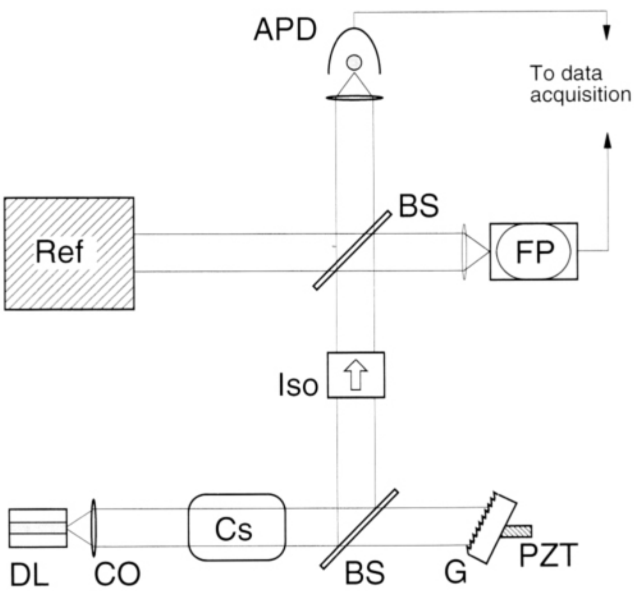

Fig. 1. Scheme of the experimental set-up. DL, diode laser; CO, collimating objective; Cs, cesium cell; BS, beam splitters; G, diffraction grating; PZT, piezoelectric transducer; Iso, magneto-optical isolator; Ref, reference diode laser; FP, scanning confocal Fabry–Perot spectrum analyzer; APD, avalanche photodiode.

The diffraction grating terminating the external cavity was mounted on a piezoelectric transducer, fixed to a mirror mounting. A continuous tuning of the laser wavelength within a range of tens of nanometers was achieved by combining the rotation of the grating and the variation of the cavity length through the piezoelectric transducer. For laser frequencies far from the Doppler-broadened absorption line of the atoms, the feedback power ratio was estimated, including losses at the optical surfaces within the external cavity, as about 30%.

In the feedback scheme considered, the light field emitted from the output facet of the diode laser, tuned to the D_2 line, passes through the atomic vapor cell as a pump field and, after being attenuated by the vapor, is retroreflected and used as a counterpropagating probe field, which is fed back into the laser cavity. At the center of any hyperfine transition of the D_2 absorption line, the pump beam bleaches a hole in the absorption spectrum of the weaker probe beam. Therefore, the probe transmission, and hence the optical feedback intensity, is resonantly enhanced when the laser frequency matches one of the principal transition or crossover lines [Schmidt *et al.*, 1994]. The saturated medium also modifies, due to its dispersive properties, the feedback phase. As an effect of the frequency-dependent changes produced by the intracavity absorber on the feedback parameters, we observed single-mode emission with frequency locking to an atomic resonance, as well as multi-mode operation with each oscillation frequency locked to a different sub-Doppler feature of the atomic absorption spectrum. This is a clear evidence of the influence of the atomic absorber on the laser operation. An extensive analysis of the results of the spectral measurements performed on this system is reported in [di Teodoro *et al.*, 1997], where a discussion of the absorption and dispersion properties of the atomic vapor under saturation spectroscopy conditions is included.

3. Temporal Dynamics and Time-Series Analysis

Mono-mode self-locked operation was obtained within a locking range of ~160 MHz around the frequency of the hyperfine transition $F = 4 \to F' = 5$. The corresponding laser emission had a stable intensity, with a low noise level. Out of the locking range, in the low-frequency direction, unstable regimes in the emitted intensity were observed. The time dependence of the laser output was detected while varying, as a control parameter, the free spectral range (FSR) of the external cavity by means of the piezoelectric transducer. Here we indicate the relative difference of external-cavity FSR with respect to the case of self-locked operation as $\Delta\nu$.

Figure 2(a) illustrates a portion of the time series of the laser output intensity $i(t)$ recorded for $\Delta\nu = 120$ MHz. The laser output experiences dropouts which decrease the absolute intensity by about 30%. The dropout pattern appears to be periodic with a time scale of about 0.1 ms. The power spectrum of the signal, calculated by fast Fourier transform (FFT), and shown in Fig. 2(b), is characterized by a few, well separated dominant features. This is consistent with the picture of a periodic signal. The observed period of the dropouts might be qualitatively associated with characteristic time scales of optical pumping processes within the absorber. For instance, the mean time for diffusion of Cs atoms at room temperature through the laser beam cross-section is of the order of tenths of millisecond [Schmidt *et al.*, 1994]. We should also notice that all documented intensity instabilities occurring in diode lasers subject to mere optical feedback from an external reflector take place on a much faster time scale. For example, in the regime of feedback intensity adopted in our experiment, extended-cavity diode lasers without absorber typically exhibit dropouts of the output intensity, called low-frequency fluctuations (LFF), characterized by a mean repetition rate of hundreds of MHz [Cerboneschi *et al.*, 1993]. The intensity dropouts in Fig. 2(a) resemble, in shape, the LFF dropouts. However, in addiction to the difference in time scale, a clear distinction of the self-pulsing phenomenon detected in our system with respect to LFF is the periodicity. In fact, LFF appear as intensity fluctuations irregularly spaced in time and their phase-space dynamics is very complex and described in terms of chaotic itinerancy [Sano, 1994]. Sub-nanosecond dynamics, which is not detectable with our measuring equipment, is also involved in the low-frequency fluctuation regime [Fischer *et al.*, 1996].

The time series of the output laser intensity have been processed with the time-delay method [Packard *et al.*, 1980]. Let $i(t)$ be the time dependent laser intensity, measured at equal sampling

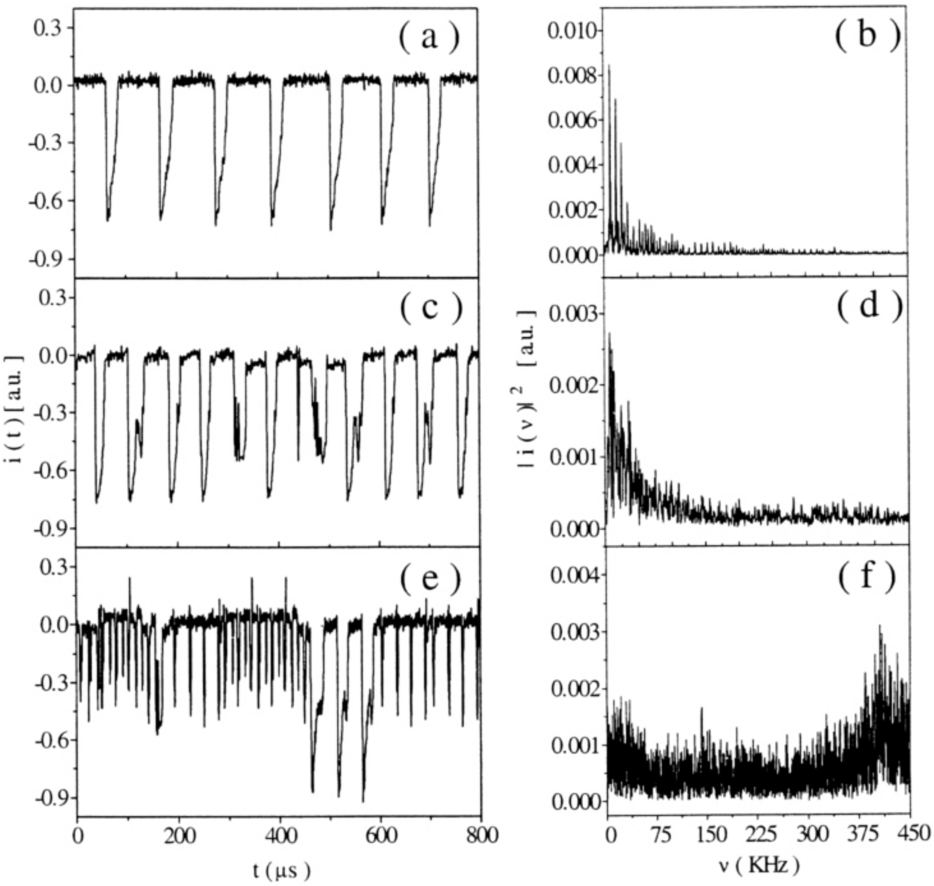

Fig. 2. Laser intensity time-series (left-hand column) and corresponding power spectra (right-hand column): (a) and (b) $\Delta\nu = 120$ MHz, (c) and (d) $\Delta\nu = 140$ MHz, (e) and (f) $\Delta\nu = 200$ MHz.

intervals δ in the temporal window $(0, \tau)$, where, for the signals recorded in our experiment, $\delta = 2\ \mu$s and $\tau = 32$ ms. A portrait of the phase trajectory of the system is represented by the set of m-dimensional embedding vectors $\mathbf{I}_n^T$, defined as

$$\mathbf{I}_n^T = \{i(n\delta),\, i(n\delta + T), \dots,\, i[n\delta + (m-1)T]\}, \quad n = 0, \dots, S, \tag{1}$$

where the lag parameter T is an integral multiple of the sampling interval δ and $S = [\tau - (m-1)T]/\delta$. In order to extract, from the time-delay portrait, both qualitative and quantitative information about the physics underlying the time series, a proper choice of m and T is needed. The algorithms applied in our analysis allowed us to test several values of m and verify the convergence of the calculated quantities for $m > 3$. The choice of parameter T was based upon the computation of the average displacement, according to the method outlined by Albano *et al.* [1988], Casdagli *et al.* [1991], and Rosenstein *et al.* [1994]. The time-delay reconstruction was utilized to calculate recurrence plots, as introduced by Eckmann *et al.* [1987]. These plots are obtained, after choosing an embedding dimension m and a suitable radius r, as a square grid of $S \times S$ elements, in which a dot is displayed at coordinate (k, n) whenever $\|\mathbf{I}_k^T - \mathbf{I}_n^T\| < r$. The embedding portrait corresponding to the time series in Fig. 2(a) is depicted in Fig. 3(a) and suggests that the dynamics of the laser intensity, in this regime, may be properly described by a limit cycle. Consistently, the recurrence plot in Fig. 3(b) belongs to the so-called periodic typology [Eckmann *et al.*, 1987], since its large-scale pattern is dominated by long lines parallel to the main diagonal, which would be the only feature in the recurrence plot of a purely oscillatory signal, superimposed to an array of regular blocks emerging from stochastic fluctuations of the characteristic frequencies.

A quantitative analysis of the time series has been performed by evaluating the largest Lyapunov

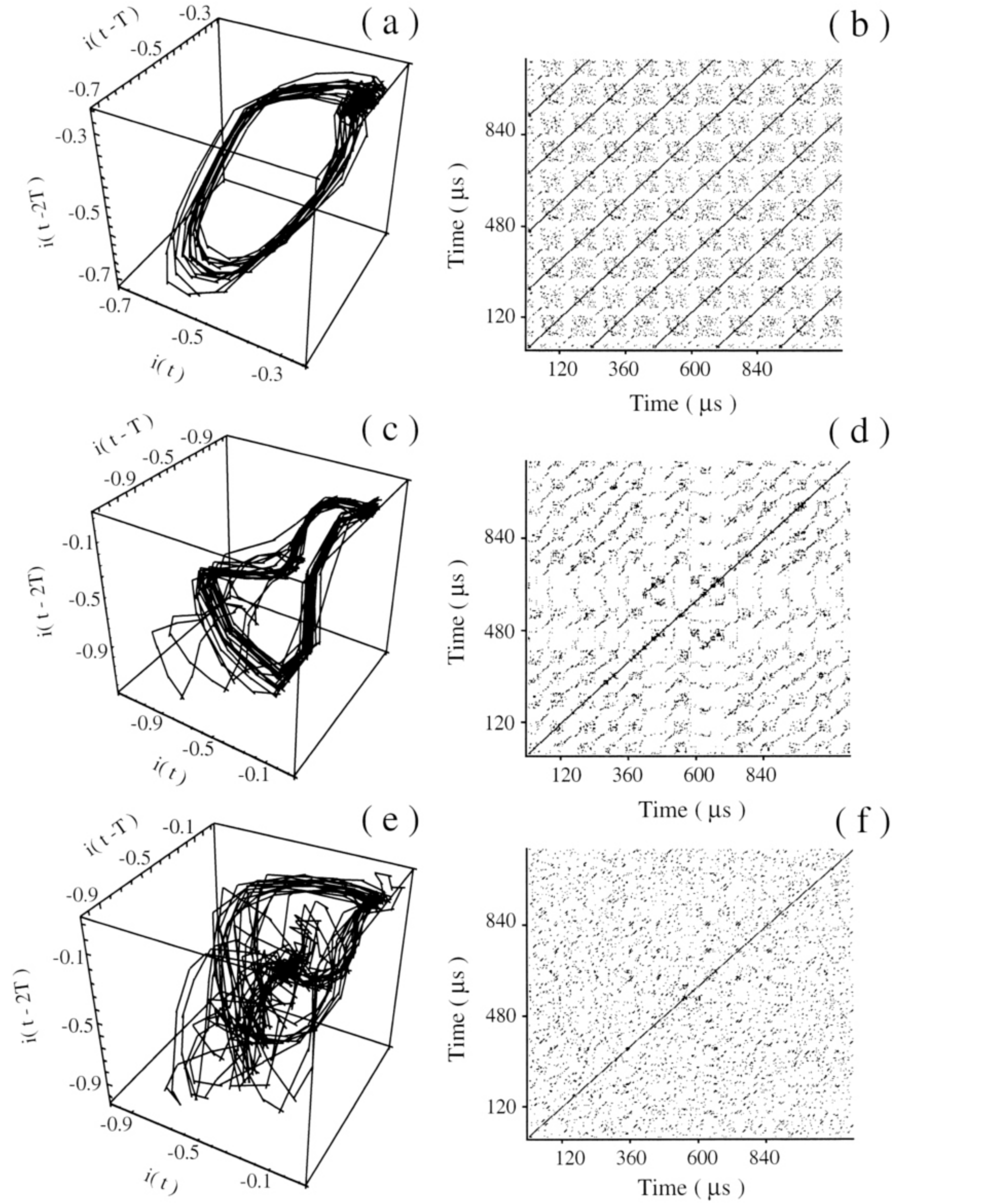

Fig. 3. Phase portraits for embedding dimension $m = 3$ (left-hand column) and recurrence plots for $m = 10$ (right-hand column) extracted from the experimental time-series: (a) and (b) $\Delta\nu = 120$ MHz, (c) and (d) $\Delta\nu = 140$ MHz, (e) and (f) $\Delta\nu = 200$ MHz. The time lag used for the phase-portraits is $T = 32$, 24, and 16 μs in (a), (c) and (e), respectively.

exponent, according to the method introduced by Rosenstein *et al.* [1993]. For the signal in Fig. 2(a), the largest Lyapunov exponent, calculated for different embedding dimensions m, is nearly equal to zero, as expected for an asymptotically stable limit cycle [Parker & Chua, 1989].

In addition, the correlation dimension D_{corr} [Grassberger & Procaccia, 1983] has been extracted

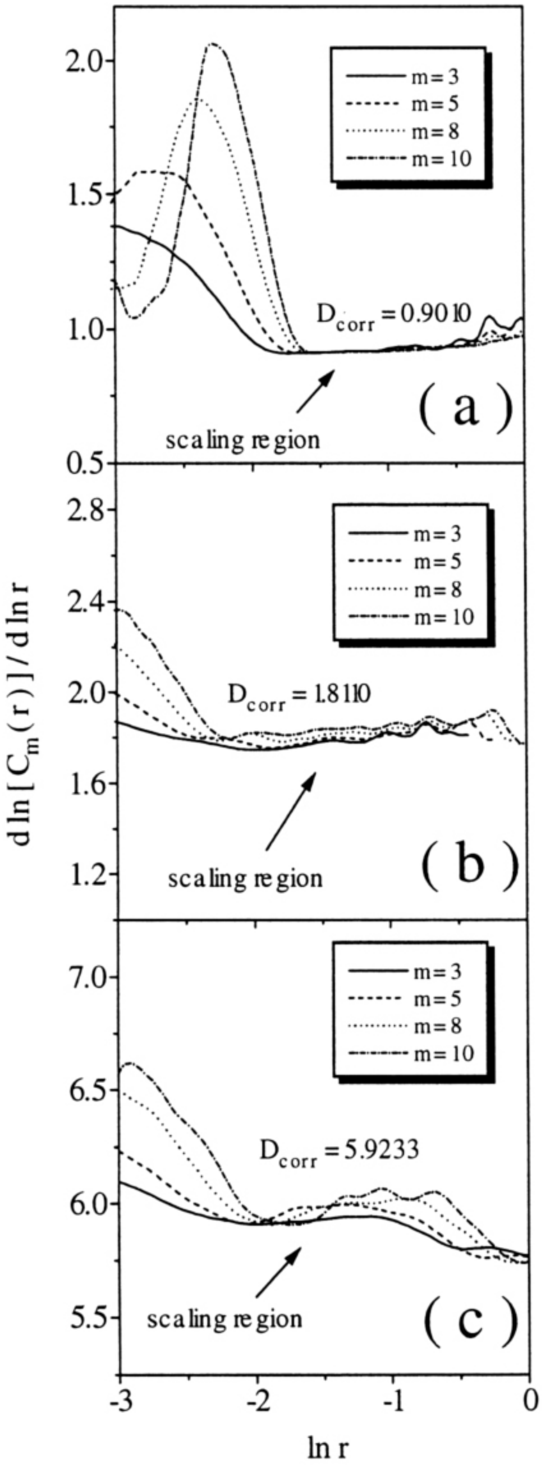

Fig. 4. Logarithmic slope of the correlation sum $C_m(r)$ as a function of $\ln r$, for several values of the embedding dimension m: (a) $\Delta\nu$ = 120 MHz, (b) $\Delta\nu$ = 140 MHz, (c) $\Delta\nu$ = 200 MHz. The height of the plateaux indicates the value of the correlation dimension D_{corr}.

from the experimental signals as

$$D_{\text{corr}} = \lim_{m\to\infty} \lim_{r\to 0} \frac{d \ln \mathcal{C}_m(r)}{d \ln r} . \qquad (2)$$

Here, the correlation sum $\mathcal{C}_m(r)$ is given by

$$\mathcal{C}_m(r) \equiv \frac{2}{S(S-1)} \sum_{\{n,k\}} \Theta(r - \|\mathbf{I}_k^T - \mathbf{I}_n^T\|) , \qquad (3)$$

where Θ is the Heavyside step-function and $\{n, k\}$ is a set of indices such that $|k-n| > t_{\text{co}}/\delta$, t_{co} being a suitable cutoff time introduced to avoid artificial correlations arising from too closely spaced embedding vectors which may result from measurements taken nearly at the same time. In our analysis, t_{co} was chosen as the inverse of the mean frequency of the power spectrum of the signal, obtained by FFT. The limit $r \to 0$ is, actually, unreliable, because small values of r are blurred by noise and limitations on experimental accuracy. In practice, a plateau referred to as scaling region should appear in the plot of $d \ln \mathcal{C}_m(r)/d \ln r$ versus $\ln r$. In Fig. 4(a), such a plot is shown, for the time series in Fig. 2(a), for several values of m and the scaling region is clearly visible. The height of the plateau represents the estimated value of the correlation dimension D_{corr}. The result obtained, $D_{\text{corr}} \simeq 1$, definitely confirms that the dynamics is described by a limit cycle.

In Fig. 2(c), part of the time series acquired for $\Delta\nu$ = 140 MHz is shown. In this case, the period fades in an irregular pattern of dropouts and the spectrum in Fig. 2(d) shows a broad-band structure. Although broad-band spectra may be associated with either stochastic or nonlinear deterministic processes, the exponential decay of the spectral intensity at high-frequencies indicates chaotic dynamics [Brandstater & Swinney, 1987]. The distortion of the phase portrait in Fig. 3(c) and the sharp change in the pattern of the recurrence plot in Fig. 3(d) support this interpretation. In particular, in the recurrence plot, the long lines parallel to the main diagonal appearing in Fig. 3(b) are now fragmented in shorter segments, the length of which has been proven to be inversely proportional to the largest Lyapunov exponent [Zbilut & Webber, 1992]. A more striking evidence of chaotic behavior is provided by the largest Lyapunov exponent, which is now positive [see Fig. 5(a)] and by the value of D_{corr} which is about 1.8 [see Fig. 4(b)].

The time series shown in Fig. 2(e) has been recorded for $\Delta\nu$ = 200 MHz. The signal shows no apparent regularity and the power spectrum in Fig. 2(f) has a broad structure which also includes additional high-frequency components. The

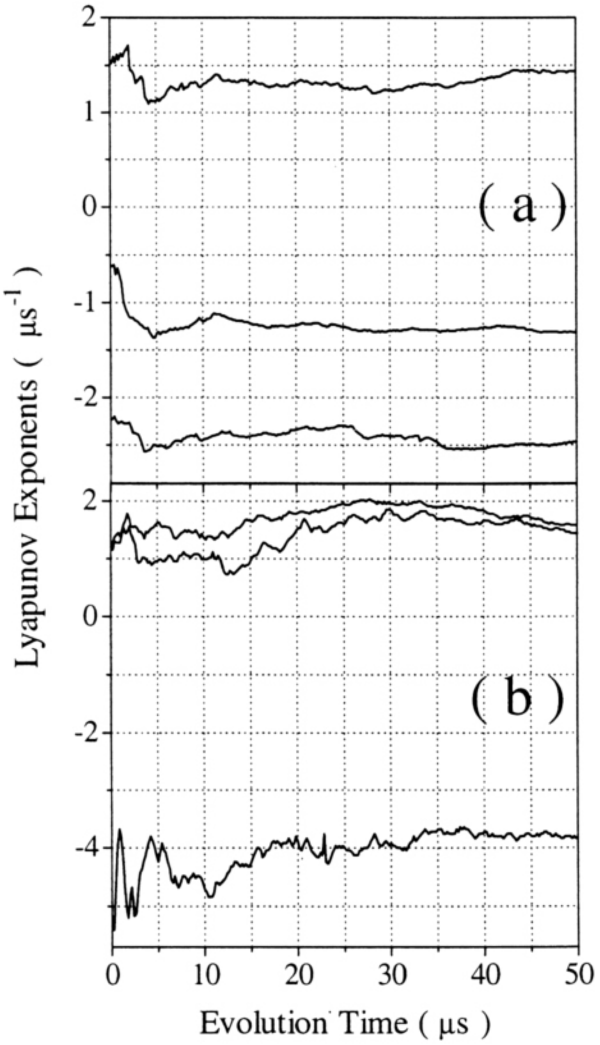

Fig. 5. Spectrum of Lyapunov exponents extracted from the time-series for $m = 3$: (a) $\Delta\nu = 140$ MHz, (b) $\Delta\nu = 200$ MHz.

phase portrait in Fig. 3(e) is markedly different from the previous ones and the trajectory explodes in a blurred and folded geometry indicating that the embedding dimension $m = 3$ used for the portrait is too low to provide reliable topological information about the laser intensity dynamics. The recurrence plot in Fig. 3(f) belongs to the homogeneous typology [Eckmann *et al.*, 1987] and any small-scale texture is hardly visible. Again, a positive largest Lyapunov exponent is found [see Fig. 5(b)] and the calculated value of D_{corr} is about 6 [see Fig. 4(c)].

The characterization of the chaotic regimes has been completed with the computation of the entire spectrum of Lyapunov exponents. For this purpose, the algorithm introduced by Darbshyre and Broomhead [1996] has been implemented in a revised and noise-robust version described by Banbrook *et al.* [1997]. The procedure has been iterated in order to obtain the evolution of the Lyapunov exponents within a certain time interval and verify their convergence. The results are shown in Fig. 5, for an embedding dimension $m = 3$. Two positive exponents have been found for $\Delta\nu = 200$ MHz and only one for $\Delta\nu = 140$ MHz. The calculation has been repeated for values of m up to 10, producing no substantial difference. Indeed, all additional Lyapunov exponents are negative in both cases.

4. Summary and Conclusions

The temporal evolution of the light emitted by a diode laser subject to feedback from an external cavity containing a cell of Cs vapor in a saturation spectroscopy configuration has been investigated experimentally. Frequency locking to the central Lamb dip of the saturated absorption spectrum of the D_2 line, accompanied by a stable laser emission has been observed. With increasing detuning $\Delta\nu$ from the atomic resonance, within the range $0 < \Delta\nu < 140$ MHz, where the laser operation appears to be strongly influenced by the presence of the atomic absorber, the output intensity displays self-pulsing and low-dimensional chaos, which take place on a time scale much longer than the time scales typical of the dynamics of a diode laser coupled to an external cavity with no absorber. For larger values of $\Delta\nu$, the laser emission shows high-dimensional chaos, characterized by two positive Lyapunov exponents. Although the presence of two positive exponents is commonly associated with hyperchaos [Rössler, 1979], it might be explained, here, in terms of coexistence of different attractors. The coexistence of attractors has been demonstrated theoretically also for diode lasers under usual feedback conditions [Masoller, 1994].

In the range of feedback strengths used in our experiment, high-dimensional chaos has been proven to underlie the dynamics of extended-cavity diode lasers with no absorber [Sano, 1994; Mirasso *et al.*, 1997]. On the other hand, our analysis suggests that a low-dimensional attractor emerges when, for relatively small detuning, the laser operation is dominated by the absorber. An interplay between different chaotic attractors might explain why no clear route to chaos has been observed. In diode lasers coupled to an external cavity with no absorber, low-dimensional chaos, reached through definite routes, has been identified in several works, as, for instance, [Mørk *et al.*, 1992; Ye *et al.*, 1993].

The time-, frequency-, and optical frequency-domain analyses performed in this paper clearly detect the same aspects of the phenomena investigated and their mutual consistency has been regarded as a significant test. The variety of dynamic regimes identified in a range of laser frequencies close to the atomic resonance, along with the ease of the experimental access to the slow absorber-induced dynamics, makes this system an interesting subject for further experimental and theoretical investigations, which would be required for a full understanding of the nonlinear and chaotic properties described here. For instance, it would be needed to explain how the characteristic time scale induced by the absorber emerges from the destabilization of the regime of self-locking.

Acknowledgments

The work of D. Hennequin at the University of Pisa was within the framework of a collaboration between the CNR of Italy and the CNRS of France.

References

Albano, A. M., Muench, J., Schwartz, C., Mees, A. I. & Rapp, P. E. [1988] "Singular-value decomposition and the Grassberger–Procaccia algorithm," *Phys. Rev.* **A38**(6), 3017–3026.

Banbrook, M., Ushaw, G. & McLaughlin, S. [1997] "How to extract Lyapunov exponents from short and noisy time series," *IEEE Trans. Signal Process.* **45**(5), 1378–1382.

Brandstater, A. & Swinney, H. L. [1987] "Strange attractors in weakly turbulent Couette–Taylor flow," *Phys. Rev.* **A35**(5), 2207–2220.

Casdagli, M., Eubank, S., Farmer, J. D. & Gibson, J. [1991] "State space reconstruction in the presence of noise," *Physica* **D51**(1–3), 52–98.

Cerboneschi, E., de Tomasi, F. & Arimondo, E. [1993] "Low frequency fluctuation instabilities in diode lasers with optical feedback," in *Nonlinear Dynamics in Lasers and Optical Systems*, ed. Mel'nikov, L. A., SPIE, Vol. 2099, pp. 183–192.

Cuneo, C. J., Maki, J. J. & McIntyre, D. H. [1994] "Optically stabilized diode laser using high-contrast saturated absorption," *Appl. Phys. Lett.* **64**(20), 2625–2627.

Darbshyre, A. G. & Broomhead, D. S. [1996] "Robust estimation of tangent maps and Lyapunov spectra," *Physica* **D89**(3, 4), 287–305.

di Teodoro, F., Cerboneschi, E., Hennequin, D. & Arimondo, E. [1997] "Multi-stability for an extended-cavity diode laser with intracavity atomic absorber," *Quantum Semicl. Opt.* **9**(5), 867–878.

Eckmann, J.-P., Oliffson Kamphorst, S. & Ruelle, D. [1987] "Recurrence plots of dynamic systems," *Europhys. Lett.* **4**(9), 973–977.

Fischer, I., van Tartwijk, G. H. M., Levine, A. M., Elsässer, W., Göbel, E. & Lenstra, D. [1996] "Fast pulsing and chaotic itinerancy with a drift in the coherence collapse of semiconductor lasers," *Phys. Rev. Lett.* **76**(2), 220–223.

Grassberger, P. & Procaccia, I. [1983] "Characterization of strange attractors," *Phys. Rev. Lett.* **50**(5), 346–349.

Kitching, J., Boyd, R., Yariv, A. & Shevy, Y. [1994] "Amplitude noise reduction in semiconductor lasers with weak, dispersive optical feedback," *Opt. Lett.* **19**(17), 1331–1333.

Liu, Z. D., Bloch, D. & Ducloy, M. [1994] "Absolute active frequency locking of a diode laser with optical feedback generated by Doppler-free collinear polarization spectroscopy," *Appl. Phys. Lett.* **65**(3), 274–276.

Masoller, C. [1994] "Coexistence of attractors in a laser diode with optical feedback from a large external cavity," *Phys. Rev.* **A50**(3), 2569–2578.

Mirasso, C. R., Mulder, M., Spoelder, H. J. W. & Lenstra, D. [1997] "Visualization of the 'Sisyphus' attractor," *Comput. Phys.* **11**(3), 282–286.

Mørk, J., Tromborg, B. & Mark, J. [1992] "Chaos in semiconductor lasers with optical feedback: Theory and experiment," *IEEE J. Quantum Electron.* **28**(1), 93–108.

Packard, N. H., Crutchfield, J. P., Farmer, J. D. & Shaw, R. S. [1980] "Geometry from a time series," *Phys. Rev. Lett.* **45**(9), 712–716.

Parker, T. A. & Chua, L. O. [1989] *Practical Numerical Algorithms for Chaotic Systems* (Springer-Verlag, Berlin) Chapter 3, p. 70.

Rosenstein, M. T., Collins, J. J. & De Luca, C. J. [1993] "A practical model for calculating largest Lyapunov exponents from small data sets," *Physica* **D65**(1, 2), 117–134.

Rosenstein, M. T., Collins, J. J. & De Luca, C. J. [1994] "Reconstruction expansion as a geometry-based framework for choosing proper delay times," *Physica* **D73**(1, 2), 82–98.

Rössler, O. E. [1979] "An equation for hyperchaos," *Phys. Lett.* **A71**(2, 3), 155–157.

Sano, T. [1994] "Antimode dynamics and chaotic itinerancy in the coherence collapse of semiconductor lasers with optical feedback," *Phys. Rev.* **A50**(3), 2719–2726.

Schmidt, O., Knaak, K.-M., Wynands, R. & Meschede, D. [1994] "Cesium saturation spectroscopy revisited:

How to reverse peaks and observe narrow resonances," *Appl. Phys.* **B59**(2), 167–178.

Ye, J., Li, H. & McInerney, J. G. [1993] "Period-doubling route to chaos in a semiconductor laser with weak optical feedback," *Phys. Rev.* **A47**(3), 2249–2252.

Zbilut, J. P. & Webber, C. L. [1992] "Embeddings and delays as derived from quantification of recurrence plots," *Phys. Lett.* **A171**(3, 4), 199–203.